

EFFECTIVE NON-OSCILLATORY PROPAGATOR FOR FEYNMAN PATH INTEGRATION IN REAL TIME

Nancy MAKRI¹

*Department of Chemistry, University of California,
and Materials and Chemical Sciences Division, Lawrence Berkeley Laboratory, Berkeley, CA 94720, USA*

Received 21 April 1989

By exploiting the momentum space boundedness of wavefunctions an effective system-specific real-time propagator is constructed, which is localized and devoid of fast oscillations. Numerical examples are presented, which show that this effective propagator can be used successfully for studying the dynamics of quantum systems with the standard Monte Carlo path integration methodology.

1. Introduction

In recent years, Feynman path integration [1] has found extensive use in the study of equilibrium statistical mechanical properties. Discretization of the integration variables on a grid converts the path integral into matrix multiplication [2], an iterative scheme which is very efficient for systems of only a few degrees of freedom. Many-body problems cannot be dealt with the above technique, though, as the size of the coordinate grid grows exponentially with the number of degrees of freedom. Monte Carlo methods [3], which are specifically designed to handle multidimensional integrals, provide an efficient tool in that case and have been successfully used in statistical mechanical calculations.

However, the above methodology is much less straightforward to apply for studying dynamical properties. Although the path integral formalism for the real time propagator, $\exp(-iHt/\hbar)$, is identical to that for the Boltzmann operator, $\exp(-\beta H)$, the standard coordinate representation of the former is highly oscillatory. Matrix multiplication is then inappropriate as a propagation scheme. There exist numerical techniques that propagate a wavefunction on a grid using the fast Fourier transform (FFT) method [4-6], and which are very efficient for problems of only a few degrees of freedom. For multidimensional systems, though, Monte Carlo path integration provides the only known alternative. Unfortunately, ordinary importance sampling methods cannot be used to evaluate the rapidly oscillatory integrals encountered in dynamical calculations. Approximate techniques for performing integration of oscillatory integrands by using the existing Monte Carlo methodology have recently been developed [7-9]. These methods introduce a weighting function which is constructed to sample primarily about the stationary phase points of the integrand, and they show promise for studying the real-time dynamics of chemical systems.

The purpose of this paper is to describe a new approach to real-time path integration. It is shown that the highly oscillatory behavior of the short-time propagator in its standard (coordinate) representation can be eliminated if the properties of the wavefunction are properly exploited. An effective system-specific real-time propagator is obtained, which is localized and devoid of rapid oscillations. This effective propagator is thus well suited for straightforward Monte Carlo path integration. The method is strictly quantum mechanical and yet very easy to implement. Another attractive feature of this approach is that its convergence characteristics

¹ Address after September 1, 1989: Department of Chemistry, Harvard University, Cambridge, MA 02138, USA.

are determined from the Fourier spectrum of the wavefunction in a simple and straightforward way.

Section 2 describes the idea and constructs the new effective propagator. Some numerical examples which illustrate the properties of this propagator are presented in section 3, and conclusions regarding the possible applications of the method appear in section 4.

2. The effective propagator

Suppose we wish to propagate an initial state $|\Psi(0)\rangle$ for a short time t by performing a single-step path integral. The procedure is expressed formally by inserting a complete set of position eigenstates between the time evolution operator and the initial state ket:

$$\langle x|\Psi(t)\rangle = \int_{-\infty}^{\infty} dx' \langle x|\exp(-iHt/\hbar)|x'\rangle \langle x'|\Psi(0)\rangle. \quad (1)$$

This is the traditional idea which, when used repeatedly, leads to the notion of an "integral over all paths". Unfortunately, the coordinate matrix element of the propagator in the previous equation is a rapidly oscillatory function of x' - behaving as $\exp[(i/\hbar)(m/2t)(x-x')^2]$ through leading order - and thus numerical integration of eq. (1) is a demanding task, particularly so if t is small. Since all known approximations to the coordinate representation of the propagator are only valid for short time, the problems associated with the numerical evaluation of a path integral become apparent.

However, it is clear that the highly oscillatory character of the propagator in the previous equation comes from the large momentum components that are present in the Fourier spectrum of the latter,

$$\langle x|\exp(-iHt/\hbar)|p\rangle = \int_{-\infty}^{\infty} dx' \langle x|\exp(-iHt/\hbar)|x'\rangle \langle x'|p\rangle. \quad (2)$$

Noting that the propagator in eq. (1) multiplies the wavefunction $\langle x'|\Psi(0)\rangle$, whose Fourier transform has a finite range (typically decaying exponentially with the momentum), we define an *effective propagator* as

$$\langle x|\exp(-iHt/\hbar)|x'\rangle_{\text{eff}} = \int_{-p_{\text{max}}}^{p_{\text{max}}} dp \langle x|\exp(-iHt/2\hbar)|p\rangle \langle p|\exp(-iHt/2\hbar)|x'\rangle. \quad (3)$$

In this, p_{max} is a cutoff momentum value, specified by the momentum space initial wavefunction according to the desired accuracy. Wavefunctions usually spread in position space under propagation, which makes their Fourier transform a narrower function as the time progresses. Convergence is easily tested by increasing the cutoff value p_{max} . The finite momentum cutoff is also introduced numerically in the FFT algorithm [4,5]; in this paper, though, we use this feature to obtain an analytic expression for the coordinate representation of the propagator. In light of the above argument, this effective propagator is expected to exhibit smooth behavior for finite values of p_{max} .

There are many ways of obtaining the mixed representation propagator $\langle x|\exp(-iHt/\hbar)|p\rangle$ that appears in eq. (3) to lowest order in the time t . An approach that can be made more accurate in a simple and systematic way is to view the x - p propagator as a time-evolved plane wave, whose short-time evolution is well approximated by an exponential power series in time. The procedure for determining the coefficients of this series for a general wavefunction is outlined in the appendix. Assuming a one-dimensional Cartesian Hamiltonian of the form

$$H = p^2/2m + V(x), \quad (4)$$

the result for the propagation of a plane wave (i.e. the mixed propagator) through order t is

$$\langle x | \exp(-iHt/\hbar) | p \rangle = \left(\frac{1}{2\pi\hbar} \right)^{1/2} \exp \left\{ \frac{i}{\hbar} \left[px - \left(\frac{p^2}{2m} + V(x) \right) t \right] \right\}. \quad (5)$$

Higher-order terms are easy to obtain, and the multidimensional generalization is straightforward. The second factor in eq. (3) is easily obtained from eq. (5) by invoking time reversal symmetry arguments, i.e. by replacing t by $-t$ and complex conjugating.

It is useful to obtain an explicit formula for the effective propagator, and for this purpose we integrate eq. (3) analytically. The integration is possible because the exponent of the mixed propagator (cf. eq. (5)) is *quadratic* in p . (This is actually true up to order t^3 .) The result is

$$\langle x | \exp(-iHt/\hbar) | x' \rangle_{\text{eff}} = \left(\frac{m}{2\pi i \hbar t} \right)^{1/2} \exp \left[\frac{i}{\hbar} \left(\frac{m}{2t} (x-x')^2 - \frac{1}{2} t [V(x) + V(x')] \right) \right] f_{\text{smooth}}(x-x'; p_{\text{max}}; t) \quad (6a)$$

with f_{smooth} given by

$$f_{\text{smooth}}(x-x'; p_{\text{max}}; t)$$

$$= \frac{1}{2} \left\{ \text{erf} \left[\left(\frac{it}{2m\hbar} \right)^{1/2} p_{\text{max}} + \left(\frac{im}{2\hbar t} \right)^{1/2} (x-x') \right] + \text{erf} \left[\left(\frac{it}{2m\hbar} \right)^{1/2} p_{\text{max}} - \left(\frac{im}{2\hbar t} \right)^{1/2} (x-x') \right] \right\}, \quad (6b)$$

where $\text{erf}(z)$ is the error function of complex argument [10],

$$\text{erf}(z) = \frac{2}{\pi^{1/2}} \int_0^z \exp(-x^2) dx.$$

The first factor in eq. (6a) is recognized as the standard expression for the coordinate representation of the propagator, which is obtained by using the Trotter product rule. The part involving the error functions (the *smoothing factor*), though, is the new result of this section. It is this part of the effective propagator that smooths out the oscillations present in the kinetic energy part of the Trotter propagator. It is easy to check that eq. (6a) reduces to the standard Trotter form of the short-time propagator if $p_{\text{max}} \rightarrow \infty$:

$$\lim_{p_{\text{max}} \rightarrow \infty} \langle x | \exp(-iHt/\hbar) | x' \rangle_{\text{eff}} = \left(\frac{m}{2\pi i \hbar t} \right)^{1/2} \exp \left[\frac{i}{\hbar} \left(\frac{m}{2t} (x-x')^2 - \frac{1}{2} t [V(x) + V(x')] \right) \right]. \quad (7)$$

To establish the properties of this effective propagator, it is useful to distinguish between two cases:

(a) For points x' sufficiently far from x , such that

$$(m/t) |x-x'| \gg p_{\text{max}} \quad \text{and} \quad (m/\hbar t)^{1/2} |x-x'| \rightarrow \infty \quad (8a)$$

(the *classically inaccessible region*), one can use the asymptotic properties of the error function [10] to show that the smoothing factor of eq. (6) is proportional to

$$f_{\text{smooth}}(x-x'; p_{\text{max}}; t) \propto \frac{1}{x-x'} \exp \left(-\frac{i}{\hbar} \frac{m}{2t} (x-x')^2 \right) \sin [p_{\text{max}}(x-x')/\hbar]. \quad (8b)$$

The exponential factor of the above equation *cancels the fast oscillations* that arise from the kinetic energy part of eq. (6). The only oscillations that remain are of constant wavelength, and the effective propagator is *damped* as $(x-x')^{-1}$ with increasing separation of the coordinate points. These features are very useful for the purpose of numerical integration, and are illustrated in fig. 1.

(b) For x' near x , i.e. if

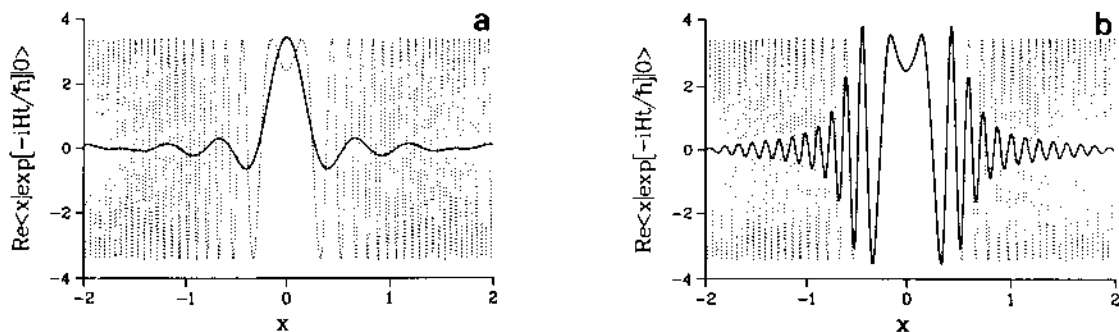


Fig. 1. Comparison of the effective propagator, eq. (6), to the standard propagator, eq. (7), for two different values of cutoff momentum p_{\max} . Plotted is the real part of the propagator with $x'=0$ as a function of x (in atomic units), for the double-well potential of eq. (11). The time step is equal to $1/40$ of the period that corresponds to the harmonic potential at the minimum. Solid line: effective propagator, eq. (7), with cutoff momentum value p_{\max} . Dotted line: standard propagator, eq. (8). (a) $p_{\max} = 12$ atomic units; this is the value which was used in the first application of section 3. (b) $p_{\max} = 48$ atomic units.

$$(m/t) |x-x'| < p_{\max} \quad (9a)$$

(the classically accessible region), one can only use the asymptotic behavior of the error function if

$$(t/\hbar m)^{1/2} p_{\max} \gg 1. \quad (9b)$$

This is the case with large time increment t , large momentum cutoff p_{\max} , or small \hbar . Then the smoothing factor approaches unity and the effective propagator behaves like the standard short time propagator. If one were to integrate eq. (6) over x' in order to propagate a wavefunction, stationary phase points would occur whenever

$$(m/t)(x-x') = -\frac{1}{2}tV'(x'), \quad (9c)$$

i.e. on the classical path. (Points x' that satisfy eq. (9c) but do not lie within the range dictated by eq. (9a) are to be ignored. Phrased in different words, this fact states that classical paths of momentum higher than p_{\max} are not allowed in the present situation.)

Fig. 1 shows the real part of the effective propagator, eq. (6), with $x'=0$, for the case of a double-well potential (see section 3) with a typical time step and for two different cutoff values p_{\max} . For fig. 1a, p_{\max} was chosen based on the momentum distribution of the initial state that was used in the first numerical example of section 3. In fig. 1b, a much larger value of p_{\max} was used. The behavior described above is clearly seen. The standard Trotter propagator, eq. (7), is also shown in the same figures for comparison. It is interesting to point out that the asymptotic property, eq. (8a), is satisfied faster for shorter t . This means that the above behavior is approached for relatively small separations $x-x'$ if the time increment is small.

Consider now using the effective propagator, eq. (6), to evaluate a path integral by Monte Carlo methods. Since the damping of the integrand at large separation is built in the propagator, one can multiply and divide the integrand by a function

$$F(x, x') = (\lambda/\pi)^{1/2} \exp[-\lambda(x-x')^2], \quad (10)$$

which is to be used as the sampling function. The parameter λ is chosen such that eq. (10) resembles the true $(x-x')^{-1}$ behavior of the integrand as closely as possible over a fixed interval which is determined to be important in the integration. Since this weighting function is normalized, one need not calculate normalization integrals numerically [8].

Comparison of the method proposed here with stationary phase based Monte Carlo schemes [7-9] is ap-

propriate at this point. When the standard highly oscillatory expression, eq. (7), is used as the short-time propagator in a path integral, *all* conceivable paths that connect the given initial and final points contribute with the *same absolute weight* (probability) but different phases. The numerical value of the integral is then the result of enormous cancellation, with the dominant contributions coming from the stationary phase regions of the integrand, which correspond to classical paths. If, on the other hand, the effective short-time propagator of eq. (6) is used instead, then phase cancellation is a relatively unimportant issue in determining the numerical value of the result. The reason for this is that different paths are *weighted differently* and give rise to slowly varying phases in the present case. Thus, short paths tend to dominate, as they enter the path integral with relatively large probability, while paths involving steps of large momentum contribute with much smaller absolute weight. Classical paths of the latter type (i.e. of high kinetic energy) have essentially zero contribution, and short classical paths are not treated more favorably than other short paths. Stated more explicitly, in the present method one sums over *all* paths that are allowed by the momentum range of the wavefunction. This is feasible, provided that the effective propagator is not rapidly oscillatory in the region where it has significant amplitude. The fact that it is not necessary to exclude non-classical-like paths from the summation means that *quantum effects are fully accounted for* when the effective propagator of eq. (6) is used.

It is also of interest to point out a remote connection of the present approach with the partial averaging technique of ref. [11]. According to the partial averaging method, one tries to include paths of high-frequency Fourier components in order to obtain a more accurate short-time propagator. In the approach taken here, though, one eliminates all large momentum components from the effective propagator, knowing that their contribution is exponentially small when the propagator is multiplied by a wavefunction with a bound Fourier spectrum.

The efficiency of the scheme suggested above depends heavily on how smoothly the effective propagator behaves in the "classically accessible region". It is not hard to show that the generic behavior of the effective propagator is that indicated in fig. 1a, i.e. the "asymptotic region" where the propagator is damped has been reached by the time *only one* or so phase oscillation has been completed, as long as the problem belongs to the quantum regime (small quantum numbers). To illustrate this we examine the $\hbar \rightarrow 0$ limit of the effective propagator when the quantum number of the state is held fixed, noting that in that limit the cutoff momentum p_{\max} also vanishes. (This is so because the phase space volume $\Delta x \Delta p$ occupied by a quantum state is (for one degree of freedom) proportional to Planck's constant. (Here Δx and Δp can be defined as the distance between classical turning points in position and in momentum space, respectively.) Typically (e.g. for a harmonic potential) $\Delta x \propto \hbar^{1/2}$ and $\Delta p \propto \hbar^{1/2}$, which implies that $p_{\max} \propto \hbar^{1/2}$.) It then follows that for time increment smaller than the period corresponding to the shortest time scale of the problem, the change in the action through the entire "classically accessible region" of eq. (9a) (beyond which the effective propagator is damped) is only of order \hbar .

We thus anticipate the effective propagator of eq. (6) to be most useful in situations where quantum effects are large. Such cases are intimately connected with the existence of coalescing or complex stationary phase points of the integrand and tend to render stationary phase based approximations inaccurate. In the opposite limit, where classical mechanics plays the principal role in determining the dynamics (e.g. with highly excited states or with very harmonic-like potentials), semiclassical approximations are already quite accurate; in such cases calculation of quantum corrections using stationary phase Monte Carlo methods should be an easier task than attempting to obtain the full quantum solution directly according to the method described in this section, which is not biased toward sampling near classical paths.

Finally, we point out that the analytic integration of eq. (3) can be performed as easily with the propagator of eq. (5) including terms up to order t^3 . This results in more accurate expressions, and also brings derivatives of the potential in the arguments of eq. (6). The resulting propagator can then be used for evaluation of a path integral using Metropolis sampling techniques.

3. Numerical applications

In this section we present several numerical calculations that illustrate the features of the effective propagator discussed in section 2 and its usefulness for evaluating path integrals by Monte Carlo methods.

The most important property of the effective propagator is that it is localized and relatively smooth. To demonstrate this we first use it to propagate a wavefunction according to the matrix multiplication scheme [2]. Specifically, a vector containing the values of the wavefunction at selected grid points is generated at each time step; this vector is then multiplied by the propagator matrix, to yield the wavefunction vector at the next time increment. This is equivalent to doing a path integral but has the advantage of being free of statistical error, thus permitting unambiguous assessment of the accuracy of the method.

For the first application, a Gaussian wavepacket is propagated in a one-dimensional symmetric double-well potential of the form

$$V(x) = -\frac{1}{2}a_0x^2 + \frac{1}{4}c_0x^4, \quad (11)$$

with the parameters chosen such that the mass is that of a hydrogen atom and the barrier height is approximately 4 kcal/mol. The initial Gaussian wavepacket is centered at one minimum of the double well and has a width equal to that of the ground state of the local harmonic approximation to the potential. The duration of the tunneling process corresponds to many vibrational periods. Wavefunction was propagated for a full tunneling period using the effective propagator of section 2 with the time step equal to about 1/40 of the harmonic vibrational period and the results were compared to those of numerically exact calculations performed by standard basis set methods. (Such short time step was necessary in order to obtain results of the accuracy mentioned below for time as long as a full tunneling period.) A grid of only 25 points was used to span the x coordinate. Had we used the standard coordinate propagator instead of the effective propagator of section 2, hundreds of points would have been necessary to construct an adequate propagation matrix. The coordinate matrix element of the propagator that was used in the calculation with $x'=0$ is shown in fig. 1a. Fig. 2 shows the survival probability (the time autocorrelation function squared) as a function of time. The agreement of the results obtained by using the effective propagator scheme with the exact ones is seen to be excellent at all times. In fact, the results converged to three decimal figures, and arbitrary precision can be achieved by adjusting the cutoff value of the momentum range used in the calculation.

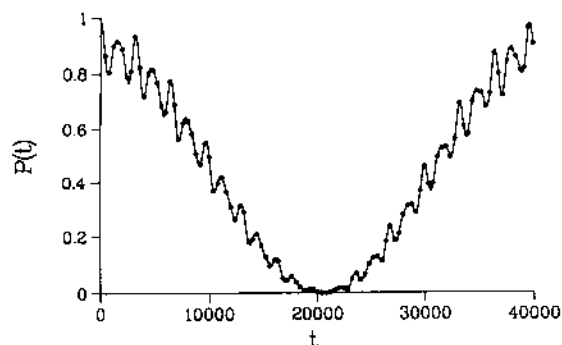


Fig. 2. The survival probability, $P(t) = |\langle \Psi(0) | \exp(-iHt/\hbar) | \Psi(0) \rangle|^2$, for a Gaussian which starts out as an eigenstate of the local harmonic approximation to the double-well potential (eq. (11)) about one minimum. The points show results obtained by propagating the wavefunction according to the matrix multiplication scheme, with time step equal to that used in fig. 1. Exact results, obtained by a basis set calculation, are indicated by the solid line for comparison.

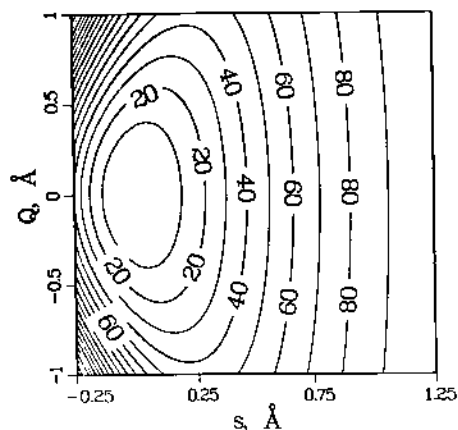


Fig. 3. Contour plot of the two-dimensional potential that describes the dynamics of energy flow between the CH stretch and the CCH in-plane wag in benzene (cf. eq. (12)). The numbers labeling the curves indicate the height of the potential surface in kcal/mol.

The second example involves a two-dimensional model that describes the dynamics of energy transfer between the CH stretch and the CCH in-plane wag in benzene. For quantum numbers $v=4-8$, where broad spectra are observed experimentally, the process takes place via a Fermi-resonance-type interaction [12] and the local-mode picture is appropriate. Our model potential has the form

$$V(s, Q) = D[1 - \exp(-as)]^2 + \frac{1}{2}m_Q\omega_0^2 \exp(-cs)Q^2. \quad (12)$$

Here s represents the CH stretch coordinate and Q the CCH in-plane wag, with the parameters chosen to fit those of ref. [12]. A contour plot of the potential is shown in fig. 3.

In order to test the ability of the present method to accurately describe the dynamics of energy flow, we propagate an initial state which is an eigenstate of the uncoupled ($c=0$) Hamiltonian with four quanta in the CH oscillator. Fig. 4 shows the survival probability as a function of time and compares with exact results obtained by a basis set calculation.

Finally, we present a path integral calculation of the survival probability for a Gaussian wavepacket in a one-dimensional Morse potential,

$$V(x) = D[\exp(-2\alpha x) - 2\exp(-\alpha x)], \quad (13)$$

with $D=0.164$ and $\alpha=0.9374$ in atomic units (see also ref. [6]), using the Monte Carlo integration scheme. The parameters are chosen to correspond roughly to the vibrational motion of H_2 , i.e. the well depth is 4.46 eV and the harmonic frequency at the minimum is 3910 cm^{-1} . The initial wavepacket is displaced by -0.1 \AA from the equilibrium position and has width which corresponds to the ground state of the harmonic approximation to the potential. The calculation was performed with a time step equal to about 1/10 of the vibrational period, with 100000 Monte Carlo points per integration variable. The computational details are as described in ref. [8], except that in the present case a sampling function of the type given by eq. (10) was used and thus the normalization integral [8] was obtained analytically. Fig. 5 shows the survival probability as given by the Monte Carlo calculation with the effective propagator of section 2 and compares with the exact

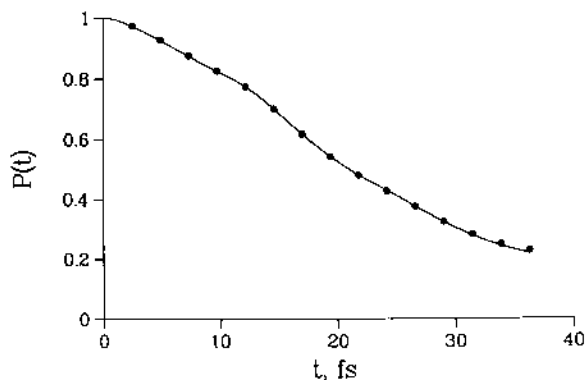


Fig. 4. The survival probability for a wavefunction in the potential of fig. 3 (eq. (12)). The initial state is an eigenstate of the uncoupled ($c=0$) Hamiltonian, with four energy quanta in the CH coordinate. The points show results obtained by propagating the wavefunction according to the matrix multiplication scheme. Exact results, obtained by a basis set calculation, are indicated by the solid line for comparison.

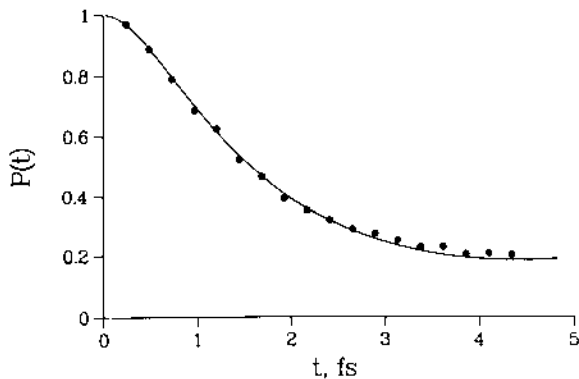


Fig. 5. The survival probability for a wavefunction in a Morse potential. The initial state is a Gaussian wavepacket which is displaced by -0.1 \AA from the equilibrium position and has width equal to that of the eigenstate of the harmonic approximation at the potential minimum. The points show results obtained by a Monte Carlo calculation using a time step equal to about 1/10 of the vibrational period with 100000 Monte Carlo points per integration variable. The Monte Carlo statistical error bars are smaller than or equal to the size of the points. The solid line shows the exact result, obtained by a basis set calculation.

results. It is seen that accurate results with reasonably small statistical error can be obtained, while an extremely simple Monte Carlo algorithm was used.

4. Discussion and concluding remarks

The analysis of section 2, along with the numerical calculations of section 3, shows that the effective propagator defined in section 2 possesses the desirable properties of localization and smooth behavior which are essential to numerical evaluation of a path integral. The most important feature is that the calculation can be arranged to give the desired accuracy by properly adjusting the cutoff value of momentum explored by the wavefunction of interest. Furthermore, the fact that the sampling function for the Monte Carlo calculation has an extremely simple form results in considerable savings, as it is analytically normalizable (a fact important in real time dynamics), and also eliminates the need for search of stationary phase points of the integrand, which is usually a demanding task. We therefore believe that the effective propagator will prove useful for studying the dynamics of multidimensional quantum systems by path integral methods.

Furthermore, we suggest that the effective propagator should also find utility in the calculation of correlation functions,

$$C(t) = \text{Tr}[\exp(iHt_c/\hbar)\hat{A}\exp(-iHt_c/\hbar)\hat{B}], \quad (14)$$

where \hat{A} and \hat{B} are quantum mechanical operators, and $t_c \equiv t - \frac{1}{2}i\hbar\beta$, with $\beta = 1/kT$. (By setting both \hat{A} and \hat{B} equal to the flux operator,

$$F = \frac{1}{2m} [\delta(\hat{s} - s_0)\hat{p}_s + \hat{p}_s\delta(\hat{s} - s_0)], \quad (15)$$

one obtains the flux correlation function [13], whose time integral yields the rate of a reactive process. In eq. (15) s is the reaction coordinate and s_0 its value at the dividing surface, i.e. the surface through which the flux is measured.)

To evaluate eq. (14) in a path integral fashion, one must be able to compute the complex time propagator. Expressing the latter as

$$\langle x | \exp(-iHt_c/\hbar) | x' \rangle = \int dx'' \langle x | \exp(-iHt/\hbar) | x'' \rangle \langle x'' | \exp(-\beta H) | x' \rangle \quad (16)$$

allows one to think of the problem in a way similar to eq. (1). Specifically, the coordinate matrix element of the Boltzmann operator that appears in eq. (16) effectively plays the role of a wavefunction [14] and thus defines a momentum cutoff value. Low temperature (large β) should be easier to deal with, as only low energy states are populated in that case. The calculation should be rather similar to the time propagation of wavefunctions treated in this paper, but numerical tests are necessary in order to assess the actual feasibility and usefulness of the method for studying non-equilibrium properties of complex systems.

Finally we wish to emphasize that the method suggested in this paper should be more difficult to implement for studying long-time dynamics, as is true of all path integral methods. (By "long time" we mean time much longer than the shortest time scale that appears in the problem, i.e. time for which many (e.g. hundreds of) time slices will be required to yield convergent results.) Apart from reasons pertaining to the dimensionality of the integral itself, which increases with the time, additional problems often arise. These are usually associated with the existence of multiple classical paths that connect the given endpoints. Stationary phase-based methods must explicitly search for these classical paths, and this is a non-trivial task. Use of the effective non-oscillatory propagator scheme excludes paths of large momentum steps but samples all paths of momentum smaller than the cutoff value. While the method does so in a very efficient way, i.e. by circumventing the problem of highly oscillatory behavior that would arise if the standard propagator were used, it is still expected that the statistical

error will grow with time, since larger fluctuations from the straight line path will then be included. The staging algorithm [15] is ideally suited for dealing with such problems, and we believe that it will help to extend the range of applicability of the effective propagator technique described in this paper to problems requiring much longer time propagation.

Acknowledgement

I would like to thank Professor William H. Miller for his encouragement and for many helpful discussions. This work has been supported by the Director, Office of Energy Research, Office of Basic Energy Sciences, Chemical Sciences Division of the US Department of Energy under Contract No. DE-AC03-76SF00098.

Appendix

Here we describe a simple recursive procedure for obtaining analytically the short-time evolution of a wavefunction in a Hamiltonian of the form

$$H = \mathbf{p}^2/2m + V(\mathbf{x}).$$

The procedure is similar to the exponential power series expansion of the propagator presented in ref. [16]. We assume that the propagated wavefunction can be written as a single exponential, i.e.

$$\Psi(\mathbf{x}, t) \equiv \exp[iW(\mathbf{x}, t)/\hbar] \quad (\text{A.1a})$$

and expand the exponent in a power series in time:

$$W(\mathbf{x}, t) = \sum_{n=0} W_n(\mathbf{x})t^n. \quad (\text{A.1b})$$

(Note that the above assumption is *not* always valid, e.g. eq. (A.1) cannot describe the evolution of a wavepacket near a turning point, where the resulting wavefunction is composed of an incident plus a reflected wave.) Substituting eq. (A.1) into the time-dependent Schrödinger equation and equating like powers of t yields the following recursion relations which determine the expansion coefficients $W_n(\mathbf{x})$:

$$W_1 = -V + \frac{i\hbar}{2m} \nabla^2 W_0 - \frac{1}{2m} (\nabla W_0)^2, \quad (\text{A.2a})$$

$$W_{n+1} = \frac{1}{n+1} \left(\frac{i\hbar}{2m} \nabla^2 W_n - \frac{1}{2m} \sum_{k=0}^n \nabla W_k \cdot \nabla W_{n-k} \right), \quad n \geq 1, \quad (\text{A.2b})$$

where W_0 is given by the logarithm of the initial wavefunction:

$$W_0 = -i\hbar \ln \Psi(0). \quad (\text{A.2c})$$

Application to the time evolution of a plane wave (see section 2) is straightforward.

References

- [1] R.P. Feynman, Rev. Mod. Phys. 20 (1948) 367;
R.P. Feynman and A.R. Hibbs, Quantum mechanics and path integrals (McGraw-Hill, New York, 1965).
- [2] D. Thirumalai, E.J. Bruskin and B.J. Berne, J. Chem. Phys. 79 (1983) 5063.

- [3] N. Metropolis, A.W. Rosenbluth, M.N. Rosenbluth, H. Teller and E. Teller, *J. Chem. Phys.* 21 (1953) 1087;
J.P. Valleau and S.G. Whittington, in: *Modern theoretical chemistry*, Vol. 5, ed. B.J. Berne (Plenum Press, New York, 1977) pp. 137-168.
- [4] M.D. Feit, J.A. Fleck Jr. and A. Steiger, *J. Comput. Phys.* 47 (1982) 412;
M.D. Feit and J.A. Fleck Jr., *J. Chem. Phys.* 78 (1983) 301;
R. Heather and H. Metiu, *J. Chem. Phys.* 86 (1987) 301;
G. Wahnstrom and H. Metiu, *J. Phys. Chem.* 92 (1988) 3240.
- [5] R. Kosloff and D. Kosloff, *J. Chem. Phys.* 79 (1983) 1823;
R. Kosloff and C. Cerjan, *J. Chem. Phys.* 81 (1984) 3722.
- [6] R. Kosloff, *J. Phys. Chem.* 92 (1988) 2087.
- [7] N. Makri and W.H. Miller, *Chem. Phys. Letters* 139 (1987) 10.
- [8] N. Makri and W.H. Miller, *J. Chem. Phys.* 89 (1988) 2170.
- [9] J.D. Doll and D.L. Freeman, *Advan. Chem. Phys.* 73 (1988) 120;
J.D. Doll, D.L. Freeman and M.J. Gillan, *Chem. Phys. Letters* 143 (1988) 277;
J.D. Doll, T.L. Beck and D.L. Freeman, *J. Chem. Phys.* 89 (1988) 5753.
- [10] M. Abramowitz and I.A. Stegun, *Handbook of mathematical functions* (Dover, New York).
- [11] J.D. Doll, R.D. Coalson and D.L. Freeman, *Phys. Rev. Letters* 55 (1985) 1;
R.D. Coalson, D.L. Freeman and J.D. Doll, *J. Chem. Phys.* 85 (1986) 4567.
- [12] E.L. Sibert, W.P. Reinhardt and J.T. Hynes, *J. Chem. Phys.* 81 (1984) 1115.
- [13] W.H. Miller, *J. Chem. Phys.* 61 (1974) 1823;
W.H. Miller, S.D. Schwartz and J.W. Tromp, *J. Chem. Phys.* 79 (1983) 4889.
- [14] B. Hellsing, A. Nitzan and H. Metiu, *Chem. Phys. Letters* 123 (1986) 523;
G. Wahnstrom and H. Metiu, *Chem. Phys. Letters* 134 (1987) 531.
- [15] M. Sprik, M.L. Klein and D. Chandler, *Phys. Rev. B* 31 (1985) 4234.
- [16] N. Makri and W.H. Miller, *J. Chem. Phys.* 90 (1989) 904.